Chapter 4

Branching in Fungal Hyphae and Fungal Tissues:
Growing Mycelia in a Desktop Computer

David Moore, Liam J. McNulty and Audrius Meskauskas

Abstract

In mycelial fungi the formation of hyphal branches is the only way in which the number of growing points can be increased. Cross walls always form at right angles to the long axis of a hypha, and nuclear division is not necessarily linked to cell division. Consequently, no matter how many nuclear divisions occur and no matter how many cross walls are formed there will be no increase in the number of hyphal tips unless a branch arises. Evidently, for the fungi, hyphal branch formation is the equivalent of cell division in animals, plants and protists. The position of origin of a branch, and its direction and rate of growth are the crucial formative events in the development of fungal tissues and organs. Kinetic analyses have shown that fungal filamentous growth can be interpreted on the basis of a regular cell cycle, and encourage the view that a mathematical description of fungal growth might be generalised into predictive simulations of tissue formation. An important point to emphasise is that all kinetic analyses published to date deal exclusively with physical influences on growth and branching kinetics (like temperature, nutrients, etc.). In this chapter we extrapolate from the kinetics so derived to deduce how the biological control events might affect the growth vector of the hyphal apex to produce the patterns of growth and branching that characterise fungal tissues and organs. This chapter presents: (i) a review of the published mathematical models that attempt to describe fungal growth and branching; (ii) a review of the cell biology of fungal growth and branching, particularly as it relates to the construction of fungal tissues; and (iii) a section in which simulated growth patterns are developed as interactive three-dimensional computer visualisations in what we call the Neighbour-Sensing model of hyphal growth. Experiments with this computer model demonstrate that geometrical form of the mycelium emerges as a consequence of the operation of specific locally-effective hyphal tip interactions. It is not necessary to impose complex spatial controls over development of the mycelium to achieve particular morphologies.

Introduction

During the life history of many fungi, hyphae differentiate from the vegetative form that ordinarily composes a mycelium and aggregate to form tissues of multihyphal structures. These may be linear organs (that emphasise parallel arrangement of hyphae):

- strands,
- rhizomorphs
- fruit body stipes,

or globose masses (that emphasise interweaving of hyphae):

Branching Morphogenesis, edited by Jamie Davies.

- sclerotia
- fruit bodies and other sporulating structures of the larger Ascomycota and Basidiomycota.

In microscope sections, fungal tissue appears to be comprised of tightly packed cells resembling plant tissue but the hyphal (that is, tubular) nature of the components can always be demonstrated by reconstruction from serial sections or by scanning electron microscopy. Clearly, hyphal cells do not proliferate in the way that animal and plant cells do.

Plants, animals and fungi are distinct eukaryotic Kingdoms and there are fundamental differences between the three Kingdoms in the way that the morphology of multicellular structures is determined. A characteristic of animal embryology is the movement of cells and cell populations. In contrast, plant morphogenesis depends upon control of the orientation and position of the daughter cell wall, which forms at the equator of the mitotic division spindle. Fungi also have walls, like plants, but their basic structural unit, the hypha, exhibits two features which cause fungal morphogenesis to be totally different from plant morphogenesis. These are that:

- hyphae extend only at their apex, and
- cross walls form only at right angles to the long axis of the hypha.

One consequence of these "rules" is that fungal morphogenesis depends on the placement of hyphal branches. Increasing the number of growing tips by hyphal branching is the equivalent of cell proliferation in animals and plants. To proliferate, the hypha must branch, and to form an organised tissue the position of branch emergence and its direction of growth must be controlled.

Another way in which fungal morphogenesis differs from that in other organisms is that no lateral contacts between fungal hyphae analogous to the plasmodesmata, gap junctions and cell processes that interconnect neighbouring cells in plant and animal tissues have ever been found. Their absence suggests that morphogens used to regulate development in fungi will be communicated through the extracellular environment. Since published kinetic analyses deal exclusively with external influences (like nutrient status, culture conditions, etc.) on growth and branching kinetics, this encourages our view that a mathematical description of fungal vegetative growth might be generalised into predictive simulations of tissue formation, leading to better understanding of the parameters that generate specific morphologies.

Kinetics of Mycelial Growth and Morphology

Kinetic analyses show that fungal filamentous growth can be interpreted on the basis of a regular cell cycle, and in this section we review published mathematical models that attempt to describe fungal growth and branching in the vegetative (mycelial) phase.

Measurement Methodologies

Measurements of hyphal diameter, *hd*, and hyphal length, *hl*, allow hyphal volume, *hv*, to be calculated, which when multiplied by the average density of the composite hyphal material, ρ, gives an estimate of biomass, *X*. Taking these measurements over a series of time intervals enable hyphal extension rate, *E*, and the rate of increase of biomass to be calculated. Currently, automated image analysis systems permit real-time analysis of these microscopic parameters,[1] and some of these analyses suggest that hyphal tips grow in pulses,[2] although this is debatable,[3] particularly because the observations use video techniques and the pixelated image generated by both analogue and digital cameras will cause pulsation artefacts.[4]

The most important macroscopic parameter is total biomass. Total hyphal length is proportional to total biomass, if *hd* and ρ are assumed to be constant, but measurement can be difficult. Nondestructive mass measurement is rarely feasible and in most cases separating the mycelium from the substratum is difficult (and sometimes impossible). Acuña et al[5] developed a neural network that they trained to correlate colony radius with colony biomass. However, this relationship is only relevant to circular mycelia and measurements in two dimensions.

More general relationships with biomass have been suggested for particular chemical compounds, the most promising of which is ergosterol, a sterol characteristic of fungal membranes.[6,7]

Modelling Branching

A germ-tube hypha will grow in length exponentially at a rate that increases until a maximum, constant extension rate is reached. Thereafter, it increases in length linearly.[8] The primary and subsequent branches behave similarly. Trinci[9] offered a solution to the riddle of how biomass (proportional to total hyphal length) can increase exponentially when individual hyphae extend linearly by proposing that it was due to the exponential increase in tips due to branching.

Katz et al[8] studied the growth kinetics of *Aspergillus nidulans* on three different media, each with a distinct specific growth rate. From these observations they proposed a number of general relationships that are conveyed in equation (1), elucidated by Steele & Trinci:[10]

$$\overline{E} = \mu_{\max} G \tag{1}$$

where $\overline{E}$ is the mean tip extension rate, $\mu_{\max}$ is the maximum specific growth rate, and G is the hyphal growth unit. G is defined as the average length of a hypha supporting a growing tip according to equation (2):

$$G = \frac{L_t}{N_t} \tag{2}$$

where L_t is total mycelial length, and N_t is number of tips.

The hyphal growth unit is approximately equal to the width of the peripheral growth zone (more accurately, the volume of the hyphae within that zone), which is a ring-shaped peripheral area of the mycelium that contributes to radial expansion of the colony.[11,12] Hyphal tips growing outside this zone will only fill space within the colony. G is an indicator of branching density; Katz et al[8] postulated that a new branch is initiated when the capacity for a hypha to extend increases above $\overline{E}$, thereby regulating $G \approx 1$ unit.

Prosser & Trinci[13] described a model that successfully accounted for exponential growth and branching, constructed on the premise that tips extend by the incorporation into the tip membrane of new material that arrives packaged in vesicles.[14] This mechanism was modelled in two steps: (i) vesicles were produced in hyphal segments distal to the tip and were absorbed in tip segments; (ii) vesicles flowed from one segment to the next, towards the tip. Apical branching initiated when the concentration of vesicles in the tip exceeded the maximum rate that the apex could absorb the new material. Varying the ratio of these steps produced different flow rates and branching patterns. The model also incorporated the concept of the 'duplication cycle'.[15] This was achieved by increasing the number of nuclei in the model mycelium at a rate proportional to the rate of biomass increase. Septa were then assumed to form in growing hyphae when the volume of the apical compartment per nucleus breached a threshold level. This provided for initiation of lateral branches by assuming that vesicles accumulated behind septa to a concentration comparable to that which initiated apical branching. This model achieved good agreement with experimental data for total mycelial length, number of hyphal tips, and hyphal growth unit length in *Geotrichum candidum.*[13] In an adaptation of this model, Yang et al[16] used a stochastic element to account for the branching process: branching site and direction of branch growth being generated by probability functions. This gave rise to a much more realistic mycelial shape.

Describing Branching Patterns

Leopold[17] examined the generality of natural branching systems in trees and streams. Based on the classification system of Horton,[18] she labelled each branch of a tree or river network depending on how many tributary branches it supported. First-order branches have no tribu-

taries; second-order branches support only first-order branches; a third-order branch supports only first and second-order branches; etc. She also measured the lengths of each branch to obtain an average value for each order of branching (the length of an *n*-order branch includes the length of its longest (*n*-1)-order tributary). She found that straight-line plots resulted when branch order was plotted against the logarithm of (i) the number of branches of a given order, and (ii) the average length of a branch of a given order. The gradient of these lines was interpreted as (i) the branching ratio (BR = the average number of *n*-order branches for each (*n*+1)-order branch); and (ii) the length ratio (LR = the average length of each *n*-order branch as a multiple of the average length of each (*n*-1)-order branch). Observations suggest that the values of these ratios showed little variation over a range of tree species (BR = 4.7 - 6.5; LR = 2.5 - 3.6) and river networks (BR=3.5; LR=2.3).

Analysing Fungal Mycelia

Gull[19] applied Leopold's analysis to the branching characteristics of mycelia of the filamentous fungus, *Thamnidium elegans*, and observed branching and length ratios of 3.8 and 4.0, respectively, for a third-order system and 2.6 and 2.7 for a fourth-order system. Though it gave no biological insight into the mechanisms of branching, Gull's work demonstrated that mycelia employ branching as a strategy for colonising the maximum area of space using the minimum total mycelial length, and indicate that the values obtained can be interpreted as a quantification of branching frequency.

Another approach to quantifying branching frequency relies on the mathematics of fractal geometry. In the box-counting method of fractal analysis a grid of boxes, each with side length ε, is placed over the pattern, and the number of boxes, N_{box}, that are intersected by the pattern is counted. If a pattern is fractal, it will be 'self-similar' at all scales. This means that a true fractal pattern has an infinite length. However, the geometry of the pattern limits the degree to which it can fill the plane. This is quantified in terms of the fractal dimension, D, according to the formula:

$$N_{box}(\varepsilon) = C\varepsilon^{-D} \tag{3}$$

where C is a constant. A straight line has a fractal dimension, D = 1, and a completely filled plane has D = 2.

By looking at higher and higher resolutions (i.e., in the limit $\varepsilon \to 0$) the repeating pattern will be revealed to cover a limited proportion of the plane. When the logarithm of N_{box} is plotted against the logarithm of $(1/\varepsilon)$, a straight line is obtained with gradient equal to D. When applied to fungal mycelia, ε is limited by the hyphal diameter microscopically and by the mycelial diameter macroscopically. Thus, mycelia are not true fractals. However, this range is sufficient to allow reasonably accurate regression analysis for D, and thus quantification of the space filling capacity, or branching frequency, of mycelia can be obtained.

Obert et al[20] applied this method to mycelia of *Ashbya gossypii*. They found that mycelia did indeed behave as fractals, and calculated a fractal dimension, D = 1.94. Such a high value for D indicates a mature mycelium whose centre has been almost homogenously filled by branching hyphae. For the edge of mycelia they calculated D = 1.45. Thus, as a mycelium develops its fractal dimension converges towards 2 when the whole mycelium is considered and towards 1.5 when only the edge is considered. Ritz & Crawford[21] and Jones et al[22] corroborated these findings.

Matsuura & Miyazima[23] used a different form of fractal analysis to quantify the 'roughness' of the edges of mycelia grown at different temperatures and on different media. Unfavourable conditions (e.g., low temperature, low nutrient concentration or stiff media) were found to produce rough edges corresponding to a lower branching frequency.

The above analyses result in a mathematical expression of the ecological description of the dual function of the fungal mycelium: that it serves to explore, and to capture resources. A rapidly growing, sparsely branched mycelium is emphasising exploration. One in which branching density increases towards homogeneity is maximising resource capture.

Generating a Circular Mycelium

This is all well and good, but the findings could apply to a mycelium of any shape, yet the fundamental morphogenetic truth about fungi is that a germinated spore on a surface (like an agar plate) will soon produce a circular colony. Testing how circularity arises requires kinetic analyses to be elaborated into simulations and this involves more demanding calculations.

The models so far described are relatively simple kinetic descriptions that, for the most part, lend themselves to manual calculation. Cohen[24] pioneered computer analysis by devising a program that was able to generate a range of branching patterns found in the natural world from a set of simple growth and branching rules. In his model growth occurred only at the tip and branching was only initiated behind the tip. Thus, it is directly applicable to mycelial growth of most fungi. In this model growth proceeded with respect to local density fields, calculated with reference to 36 sample points spaced 10° apart around the circumference of a circle centred on a growing tip, and quantifying the pattern density in the locality. Local density minima were key parameters that directed growth into unoccupied space. Branching probability was also made a function of local density minima. A random trial incorporated into the program decided, independently, if branch initiation should occur. Finally, the direction of both growth and branching were dependent on a 'persistence factor' that quantified to what degree they continued in the same direction in spite of gradients in the density field. The persistence factor acts rather like inertia on a moving body—changes in direction are gradual rather than instantaneous. When these rules were iterated, with the persistence factor for growth nullified (i.e., growing tips proceeded in a straight line), a circular branching pattern emerged.

Hutchinson et al[25] developed this work further by applying it directly to mycelial colonies of *Mucor hiemalis*. They determined the variability of tip growth rate, distance between branches, and branching angle throughout the colonies. They were then able to fit these data to known distribution curves with defined probability density functions. Tip growth rate was found to follow a half-normal distribution, distance between branches followed a gamma distribution, and branching angle followed a normal distribution. This formed the basis for a model in which values for the three specified variables were generated from the respective probability density functions over a series of time intervals. This model generates a circular mycelium.

This came as something of a surprise because the model includes no allowances for tropic interactions between hyphae. Yet, it seems a reasonable assumption that the readily-observed fact that growing hyphae actively avoid each other (= negative autotropism, observed by Robinson,[26,27] Trinci et al[28] and Hutchinson et al[25] among others), plays a role in determining spatial organisation in mycelia, especially colony circularity.

Indermitte et al[29] constructed models of mycelial growth with the specific intention of answering the question "How does circularization happen?" Variants of the model considered cases in which behaviour was completely random; where hyphae were forbidden from crossing other hyphae; where hyphal growth direction depended on diffusion of inhibitory substances from the mycelium into the medium; and where, in addition to diffusion of inhibitory substances, growth rate depended on the rank of the branch. All variants generated circularity. Although the method by which simulations were made is not described in the paper, the authors claim that experimentation with their model indicated that tropism increased the growth efficiency, where the latter was judged by the occupation of the surface (the ratio of biomass used to area of medium covered).

It is highly significant that a purely stochastic approach can generate realistically circular colony morphology, but it does not follow that tropisms and hyphal interactions are irrelevant to modelling hyphal growth. In real life, hyphae certainly do use autotropic behaviour (positive and negative) to control spatial organisation in particular regions of the mycelium; and where the hyphal density is high, as in fungal tissues, interactions are inevitable. However, we are not convinced that the rule "crossing of hyphae is not allowed" is realistic, though it is a crucial feature of the Indermitte et al[29] model. Even a casual glance at most fungal mycelia and tissues will reveal numerous interweaving hyphae. Even the commonly-applied informal description "hyphal mat" implies a woven texture.

Tropism and Hyphal Interactions

Edelstein[30] considered such interactions, but her approach differed from the above by considering the mechanisms operating in the mycelium as a whole rather than in discrete hyphae. She assumed that growth occurred at a constant rate throughout the mycelium. This she set at μ_{max} and so also limited her model to a tangential abstraction of the growth curve. Her model owes something to Cohen[24] in that it considers the density of the mycelium with respect to space as a key feature. Two density parameters were defined:

$p = p(x,t)$ the hyphal density per unit area
$n = n(x,t)$ the tip density per unit area

and the model was then based on two partial differential equations:

$$\frac{\partial p}{\partial t} = n\overline{E} - \delta \tag{4}$$

$$\frac{\partial n}{\partial t} = \frac{\partial n\overline{E}}{\partial x} + \sigma \tag{5}$$

where $\delta = \delta(p)$ is the rate of hyphal death, $\sigma = \sigma(n,p)$ is the rate of tip creation, and $n\overline{E}$ can be considered as tip flux.

Edelstein[30] also defined, in mathematical terms, all the hyphal interactions that affect the parameter n, and which are contained in the function σ. These included both branching mechanisms, as well as tip death and tip-tip and tip-hypha anastomoses.

She then used phase plane analysis to determine which of various combinations of hyphal interactions, expressed mathematically in the function σ, had bounded non-negative solutions of equations (4) and (5). These represented combinations that yielded spatially propagating colonies. Her results showed that when $\delta = 0$, only colonies that branched dichotomously and formed tip-hypha anastomoses could propagate. However, when $\delta > 0$, most combinations of hyphal interactions yielded propagating colonies. Thus, hyphal death was shown to be an important feature of mycelial growth; in addition to the density-dependent distribution which was an initial criterion of the model.

Ferret et al[31] adopted a similar approach to Edelstein,[30] using two partial differential equations that considered parameters defined in dimensions of density. However, they sought to apply their model to bulk cultures by adjusting mean tip extension rate ($\overline{E}$) with respect to biomass, X. This adjustment was done by collecting data that quantified how E varied when two hyphae came into close proximity with each other. This effect was incorporated into the differential equation concerned with the rate of change of biomass density (proportional to hyphal-density) so that it was more likely to be applied in regions where the density of biomass was high, and had a greater effect on regions where the density of tips was high. Thus, $\overline{E}$ decreased as the mycelium grew and biomass increased. Such an approach provides an alternative to incorporating hyphal death into the model that has the advantage of also affecting $\overline{E}$, thus limiting growth in a manner typical of batch culture, and, we speculate, perhaps also hyphal masses that contribute to fruiting bodies.

All of the published work on fungal growth kinetics has been devoted to growth of mycelium, and particularly biomass production in fermenters. It is especially important that models of mycelial growth can form the foundation for modelling pellet formation in liquid media[16,32] as this can impact on the design of bioreactors, but we do not wish to examine models primarily intended for application to bulk cultures at this time. Another approach to the subject we will not deal with here considers substrate utilisation as a means of describing and quantifying the growth process, as pioneered by Monod.[33] Edelstein & Segel[34] and Mitchell,[35] amongst others, have pursued this approach successfully. This also has obvious biotechnological significance.

Opinions

In many respects the mycelium is the least interesting growth form. It is the 'default' growth mode of the fungal cell and any changes that occur in it are imposed by **external** forces (nutrients, environmental conditions, etc.). Of much greater biological interest is the way in which the 'default' growth mode might be altered by **internal** (that is, self-imposed) controls to generate the numerous differentiated cells that hyphae can produce and the native interactions between hyphae that cause them to cooperate and coordinate in the morphogenesis of fungal tissues.

Although some attempt has been made to extend the vesicle supply centre model of apical growth[14] into 2-dimensional and 3-dimensional models of apical growth and differentiation,[36,37] we are not aware of any kinetic analysis of fungal mycelial growth in three dimensions that might contribute to understanding fungal tissue morphogenesis. It is certain, though, that the equation $E = \mu G$ (Equation 1) is fundamental to understanding branching kinetics and that the ratio E/μ can tell us a lot about mycelial morphology, as it relates to the hyphal growth unit length, G, which can also be expressed as a volume.[38] Observation has shown that temperature increases do not affect G in some species. However, paramorphogens have been identified that do alter this ratio and hence G and morphology.[39] In our vector based Neighbour-Sensing mathematical model, which is introduced below, the inclusion of certain tropism vectors is also able to alter this ratio by affecting the parameter E and results in a striking array of different morphologies, some of which seem to suggest a morphogenetic process that goes beyond mycelial growth and towards differentiated tissues.

In the next section we describe briefly the sorts of tissues and hyphal interactions that must be explained eventually, and in the final section of this chapter we will describe progress in modelling key morphogenetic processes.

Construction of Fungal Tissues

Development of any multicellular structure in fungi requires modification of the normal growth pattern of a vegetative mycelium so that hyphae no longer characteristically diverge, but grow towards one another to cooperate in forming the differentiating organ.[40-42] The hyphal tip is an invasive, migratory structure. Its direction of growth after initial branch emergence must be under precise control as it determines the nature and relationships of the cells the hyphal branches will form.

Linear Organs: Strands, Rhizomorphs and Stems

Formation of parallel aggregates of hyphae (= mycelial strands and cords) is common as they provide the main translocation routes for the mycelium. They are formed in mushroom cultures to channel nutrients towards developing fruit bodies; they are also formed by mycorrhizal fungi, gathering nutrients for the host. Some fungi produce rhizomorphs, which have highly differentiated tissues and show extreme apical dominance. There is often a gradation of increasing differentiation between strand, cord (or rhizomorphs) and fruit body stipe (= stem). Linear organs arise when young branches adhere to, and grow over, an older leading hypha. From the beginning, some of the hyphae may expand to become wide-diameter but thin-walled hyphae, whilst narrow hyphal branches ('tendril' hyphae) intertwine around the inflated hyphae (Fig. 1).

Globose Structures: Sclerotia and Fruit Bodies

Sclerotia are tuber-like, with concentric zones of tissue forming an outer rind and inner medulla, with a cortex sometimes between them. They pass through a period of dormancy before utilizing accumulated reserves to 'germinate', often producing fruiting bodies immediately.

Fruiting bodies are responsible for producing and distributing spores formed following meiosis. In ascomycetes, the sexually produced ascospores are enclosed in an aggregation of hyphae termed an ascoma. Ascomata are formed from sterile hyphae surrounding the developing asci,

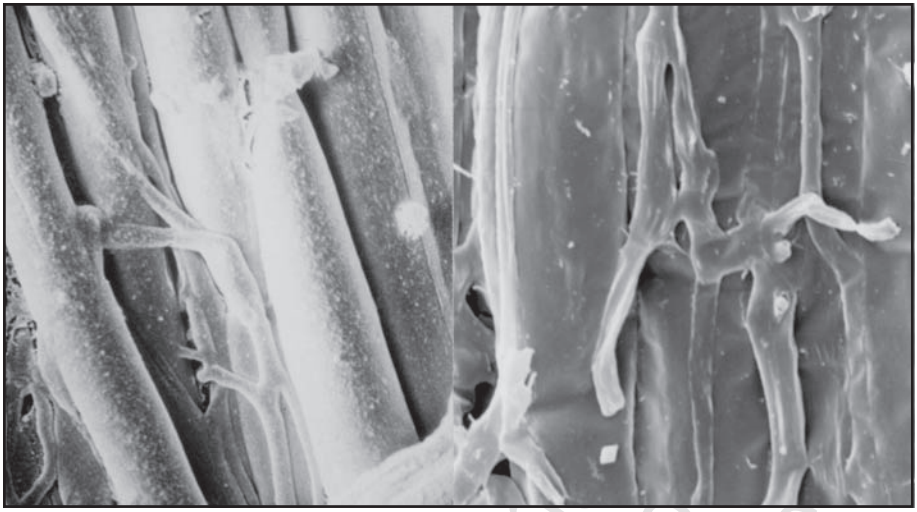

Figure 1. Two scanning electron micrographs of wide and narrow hyphae intertwined in the stem tissues of the small field mushroom, *Coprinus cinereus*. Presumably this pattern of growth is produced by positive autotropisms which ensure that the hyphae that expand to become wide diameter initially grow parallel with one another, and other tropisms that allow the narrow hyphae to grow around and intermingle with inflated hyphae.

and occur in nature in forms such as truffles and morels. The fruit-bodies of basidiomycetes, the mushrooms, toadstools, bracket fungi, puff-balls, stinkhorns, bird's nest fungi, etc., are all examples of basidiomata which bear the sexually produced basidiospores on basidia in the spore-bearing hymenial layers. These hymenia are constructed from branches of determinate growth in a precise spatial and temporal arrangement. A hyphal tip in the 'embryonic' protohymenium has a probability of about 40% of becoming a cystidium. Cystidia are large, inflated cells which are readily seen in microscope sections. When a cystidium arises, it inhibits formation of further cystidia in the same hymenium within a radius of about 30 μm. The distribution pattern of cystidia is consistent with the activator-inhibitor model that suggests that an activator autocatalyses its own synthesis, and interacts with an inhibitor that inhibits synthesis of the activator. As a result, only about 8% of the hymenial hyphal branches actually become cystidia; the rest become basidia, which proceed to karyogamy and initiate the meiotic cycle (which ends with sporulation) (Fig. 2).

Sterile packing cells, called paraphyses, then arise as branches of sub-basidial cells and insert into the hymenium (Fig. 3). About 75% of the paraphysis population is inserted before the end of meiosis, the rest insert at later stages of development. There is, therefore, a defined temporal sequence: probasidia and cystidia appear first and then paraphyses arise as branches from sub-basidial cells. Another cell type, cystesia (adhesive cells), differentiate when a cystidium grows across the gill space and contacts the opposing hymenium (Fig. 2).

Simulating the Growth Patterns of Fungal Tissues

Most models published so far simulate growth of mycelia on a single plane. However, two dimensional space has some specific peculiarities that can affect the conclusions: forbidding crossings between hyphae in the Indermitte et al models[29] being a case in point. In a real three dimensional world a large number of points can be connected without the need for the connection paths to cross; whereas the number of such points is limited on a flat plane. The need to cross will also have effect on models where patterning is based on a hyphal density field, generated by all parts of the growing mycelium, as suggested by Cohen.[24] Growth in this case is

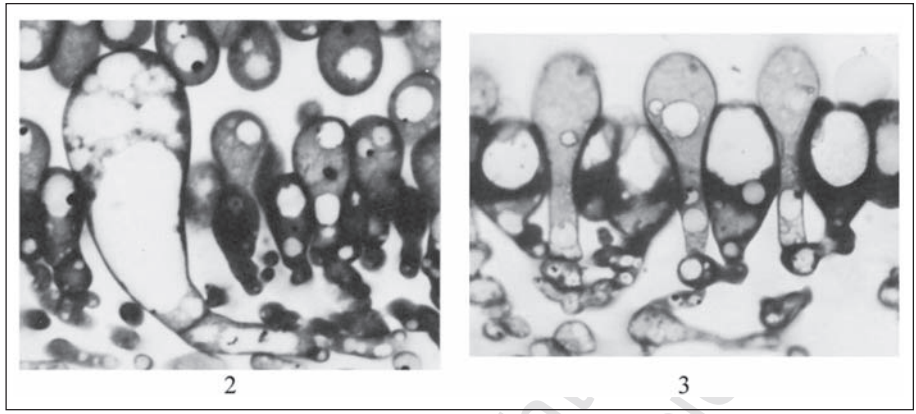

Figures 2 and 3. Light micrographs of glycolmethacrylate sections of immature hymenia of the small field mushroom, *Coprinus cinereus*. Figure 2 is the younger of the two stages shown, and the large cell in that Figure is a cystidium. Only a minority of the hyphal tips that make up the hymenium differentiate into cystidia because each cystidium establishes an inhibitory morphogenetic field around itself. Figure 3 shows that the densely-stained branches that can be seen inserting between the basidia in Figure 2, rapidly differentiate into inflated paraphyses, and in fact arise as branches from the bases of the basidia. Note also that extension growth of these hyphal tips is halted in a coordinated way so that the basidia remain as projections above the paraphyseal pavement. Overall, these images show that to construct hymenial tissue the normal divergent growth of the vegetative colony is modified to become determinate, positively autotropic, with distinctly differentiated hyphal tips of the same generation (basidia and cystidia) and distinctly different developmental fates for branches of different ranks (basidia and paraphyses).

regulated by the absolute value of this field and is directed by its gradient (equivalent to negative autotropism). In two dimensional space turning up or down is not an option, so a tip approaching an existing hypha must go across the latter, moving against a large (possibly infinite, as the distance approaches zero) value of the density field. Cohen's original model produced polarized tree-like structures, quite different from the typical spherical fungal colonies, and while the Indermitte et al models[29] succeeded in forming circular colonies, their analysis remained in two dimensions. Consequently, knowing how the circular colony arises on a flat plane is not enough; it is crucial to understand the formation of a spherical colony in three dimensional space.

Our purpose here is to suggest a model, which we call the Neighbour-Sensing model, that, whilst being as simple as possible, is able to simulate formation of a spherical, uniformly dense fungal colony in a visualisation in three dimensional space. Following Indermitte et al[29] we gauge our success on the basis that our model successfully imitates the three branching strategies of fungal mycelia illustrated by Nils Fries in 1943.[43]

Verbal Description of the Neighbour-Sensing Model

The process of simulation is defined as a closed loop. This loop is performed for each currently existing hyphal tip of the mycelium and the algorithm:

1. Finds the number of neighbouring segments of mycelium (N). A segment is counted as neighbouring if it is closer than the given critical distance (R). In the simplest case we did not use the concept of the density field, preferring a more general formulation about the number of the neighbouring tips.
2. If $N < N_{branch}$ (the given number of neighbours required to suppress branching), there is a certain given probability (P_{branch}) that the tip will branch. If the generated random number (0.1) is less than this probability, the new branch is created and the branching angle takes a random value. The location of the new tip initially coincides with the current tip. This

stochastic branch generation model is similar overall to earlier ones[16,25,44] in which distance between branches and branching angles followed experimentally measured statistical distributions. This, however, was not required to reach the desired shape of the colony in our model. Rather, we used a uniform distribution, as did Indermitte et al.[29]

We assumed that all hyphal tips in mycelia grow at constant speed. This assumption was sufficient to get the desired shape and structure of the colony.

In the simplest version, the growth direction is defined during branching and is not altered subsequently. In other words, the initial model does not implement tropic reactions (to test the kind of morphogenesis that might arise without this component). Later versions of the model tested how implementation of the density field hypothesis would affect colony growth. The density field features were made analogous to an electrical field.[24]

Implementation of a negative autotropic reaction requires the concept of the density field, as the growth must be directed by the gradient of this field. We also implemented the suggestion[24] that the tip should change direction gradually (the so-called persistence factor; see earlier section "Generating a Circular Mycelium"). In our implementation, the growth speed remained constant and the density gradient alters only the growth direction. Otherwise, a high gradient, if formed accidentally, would cause unreliably fast growth in some parts of the mycelium.

With low values of the persistence factor the model is able to form small linear structures. This is because, with such a parameter set, immediately after branching the hyphal density field tends to orient the new tip strictly in the opposite growth direction from the old tip. That is, the new hypha is directed to grow parallel with the old hypha but in the opposite direction. If we suppose that the hyphal density field is generated just by tips and branch points, this direction remains optimal until the tip goes sufficiently far from the branch point to start interacting with other hyphae. Changing parameters while the colony is still nearly linear can produce ellipsoidal or tubular structures.

We have experimented with a variety of extensions of the model (see illustrations in section "Conclusions", below): for example, growth being suppressed by a high number of neighbouring tips; or allowing the growing tip only to be active for a fixed time before it stops growing and branching. Such changes can result in more optimal packing of the hyphae, but are not required to form a spherical colony. Real fungal colonies are rarely uniform in structure, so the question arises whether any smaller new structures can form in a virtual colony growing in accordance with this model. We found that this could happen following abrupt changes of the model parameter set (especially R and N_{branch}).

Mathematical Description

Let, at the time $t \in Z_+$, the mycelium contain n growing hyphal tips. Let y_i and g_i be position and growth vectors, respectively, of the i-th growing hyphal tip at time $t \in Z_+$. Let Y be a set, containing other points of the mycelium that are sensed as neighbouring tips and/or branch points. Now, let

$$N_i = \sum_{j=1}^{n} \Phi\left(\left|y_i - y_j\right| - R\right) + \sum_{k \in Y} \Phi\left(\left|y_i - k\right| - R\right) \tag{6}$$

where Φ is a Heaviside function.

Let

$$v_i = \begin{bmatrix} \alpha_t & \beta_t & \sqrt{1-\alpha_t^2-\beta_t^2} \\ \beta_t & \sqrt{1-\alpha_t^2-\beta_t^2} & \beta_t \\ \sqrt{1-\alpha_t^2-\beta_t^2} & \alpha_t & \alpha_t \end{bmatrix}^{<Round(3\gamma_t+1)>} \tag{7}$$

where α_t, β_t and γ_t all form sequences of independent, uniformly distributed random variables over the range [0..1[.

Now compute an array b, containing all the values of i that satisfy the condition $N_i < N_{branch}$ and $\delta t < P_{branch}$. Here δt forms a sequence of independent, uniformly distributed values over the range [0..1[, and P_{branch} is the model parameter. Let m be the length of this array. For each k∈ [1..m], define:

$$y'_{n+k} = y_{b_k},\ g'_{n+k} = v(b_k) \tag{8}$$

Finally, define $y'_i = y_i + ag_i$, $g'_i = g_i$ and n′ = n+m (the model parameter *a* determines the tip growth rate in length units per defined iteration period). Define $Y' = Y + \forall y_k : k \in b$. Now we have y′, g′, n′ and Y′ defining the state of the colony after one iteration of the model algorithm.

This basic algorithm can be extended by assuming that the tip can be active only for a fixed time (S_{max} iterations) and stops growing after its length reaches L_{max} length units. Also, it could be assumed that the growth is suppressed if $N_i > N_{growth}$. To implement these extensions, let us define the age array $S(S'_i = S_i+1, S'_{n+k} = 0)$ and the length array L ($L'_i = L'_i+a$, $L'_{n+k} = 0$). Then y'_i must be redefined as $ag_i\Phi(S_i-S_{max})\ \Phi(L_i-L_{max})\Phi(N_{growth}-N_i)$ and the condition for the value, i, to join the array b must be extended to $S_i < S_{max}$. In the density field version of the model, (6) must be replaced by (9):

$$N_i = \sum_{j=1}^{n(j\neq i)} \frac{1}{\left(\left|y_i - y_j\right|\right)^2} + \sum_{k=Y}^{k\neq y} \frac{1}{\left(\left|y_i - k\right|\right)^2} \tag{9}$$

Also, N_{max} changes the biological meaning to the maximal value of the density field.

Negative autotropism was implemented using Cohen's approach.[24] In this case, v_i should be replaced by:

$$v_i = norm\left[k \cdot g_i - (1-k) \cdot norm\begin{bmatrix} \frac{d}{dy_{(i_0)}} N_i \\ \frac{d}{dy_{(i_1)}} N_i \\ \frac{d}{dy_{(i_2)}} N_i \end{bmatrix}\right] \tag{10}$$

where $norm(x) = \frac{x}{|x|}$.

Again, (6) must be replaced by (9). In (10), the parameter *k* is a model parameter, defining a particular coefficient of persistence, which is used to ensure that branches change direction gradually; and it operates on the previous growth vector g_i. The derivatives are computed by numeric differentiation. The function *norm*(x) ensures that the density gradient alters the direction but not the speed of the growth.

Implementation

Both versions of the model were implemented in Java together with the simple visualiser:

$$\forall k \in (y_i \cup Y) \exists \left\{ y_i^{screen} = \sigma k_2,\ x_i^{screen} = \sigma(k_0 \sin\alpha + k_1 \cos\alpha) \right\}$$

y_i and Y being contained in a tree-like data structure. Interactive adjustment of σ∈ [0..∞[, and σ∈ [-π..π] enabled experimental observation of the growing colony and visual appreciation of its shape. To permit examination of the internal structure of the colony, the application will display a slice of chosen thickness across the colony. This complete interactive application is available for personal experimentation at this URL: http://www.world-of-fungi.org/index.htm.

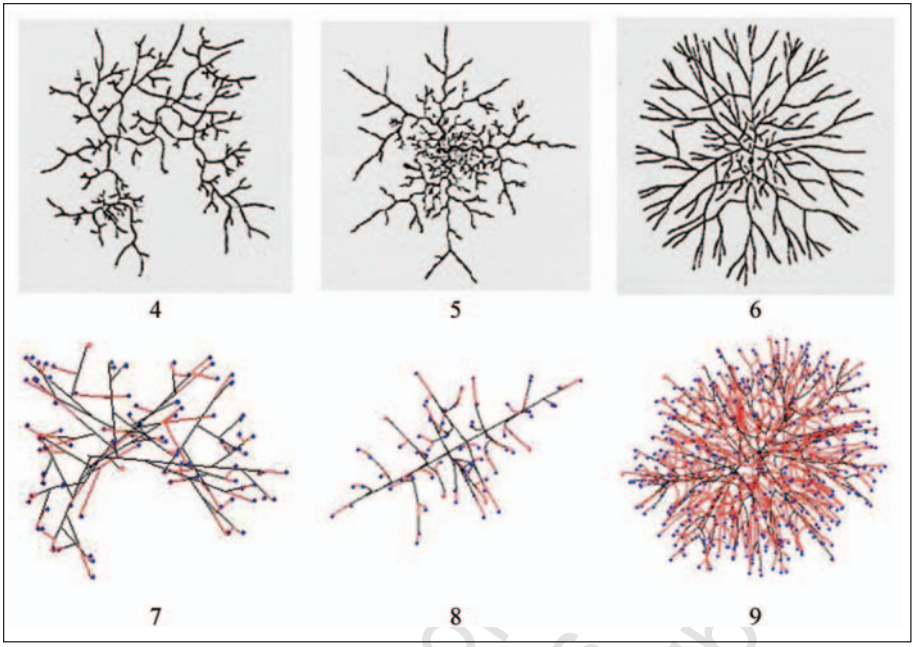

Figures 4 - 9. Comparison of three different colony types described by Fries[41] (Figs. 4 - 6) with visualisations produced by the computer model (Figs. 7-9); Figures 4 & 7 show the *Boletus* type, Figures 5 & 8 the *Amanita* type, and Figures 6 & 9 the *Tricholoma* type.

Conclusions

A random growth and branching model (i.e., one that does not include the local hyphal tip density field effect) is sufficient to form a spherical colony. The colony formed by such a model is more densely branched in the centre and sparser at the border; a feature observed in living mycelia (see earlier section "Analysing Fungal Mycelia").

Models incorporating local hyphal tip density field to affect patterning produced the most regular spherical colonies. As with the random growth models, making branching sensitive to the number of neighbouring tips forms a colony in which a near uniformly dense, essentially spherical, core is surrounded by a thin layer of slightly less dense mycelia. Using the branching types discussed by Fries[43] as our paradigm, the morphology of virtual colonies produced when branching (but not growth vector) was made sensitive to the number of neighbouring tips was closest to the so-called *Boletus* type (Figs. 4 and 7).

This suggests that the *Boletus* type branching strategy does not use tropic reactions to determine patterning, nor some predefined branching algorithm (of the sort suggested by Hogeweg & Hesper[45]). Following Occam's rule that a simpler model must be preferred if it explains the experimental data equally well,[46] we conclude that hyphal tropisms are not always required to explain "circular" (= spherical) mycelia.

When our model implements the negative autotropism of hyphae, a spherical, near uniformly dense colony is also formed, but branching is still regulated by the number of neighbouring tips (not by the density field). However the structure of such a colony is different from the previously mentioned *Boletus* type, being more similar to the *Amanita rubescens* type,[43] characterised by a certain degree of differentiation between hyphae (Figs. 5 and 8). First rank hyphae tending to grow away from the centre of the colony; second rank hyphae growing less regularly, and filling the remaining space. In the early stages of development such a colony is

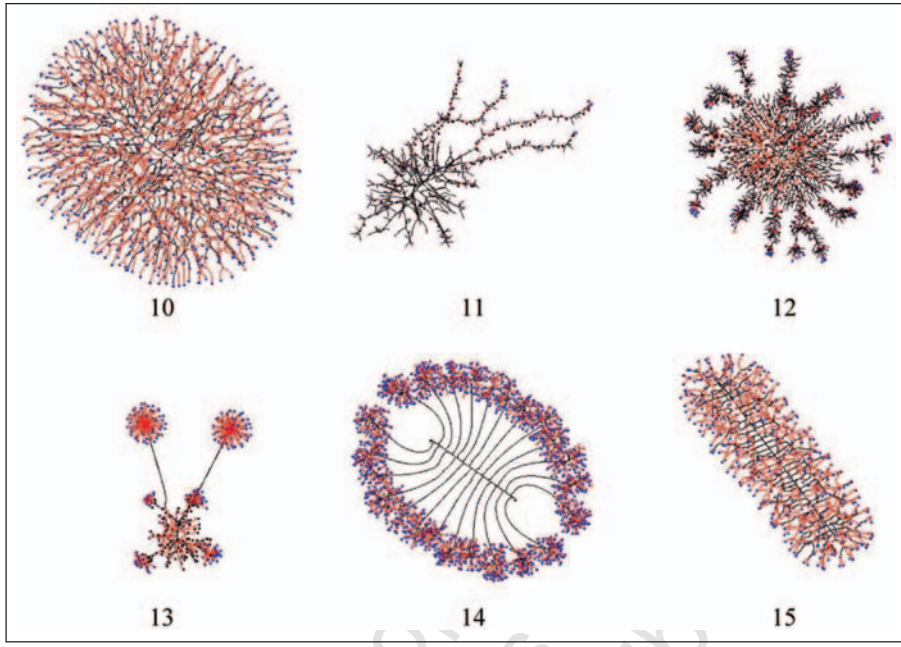

Figures 10-15. Some of the colony types obtained by varying the parameters of the model. Figure 10) *Ellipsoid*: Run for 200 time units at a growth rate of 1 length unit per time unit, with 10% negative autotropism implemented, and the density field hypothesis of branching regulation applied, where the density field threshold for branching is set at 0.1 and branching probability at 80% per time unit. Figure 11) *Mycelium with exploratory filaments*: Stage 1: Run for 100 time units at a growth rate of 1 length unit per time unit, with 10% negative autotropism implemented, and the density field hypothesis of branching regulation applied, where the density field threshold for branching is set at 0.06 and branching probability at 40% per time unit (*Tricholomas* parameter set). Stage 2: Run for 100 time units at a growth rate of 1 length unit per time unit, with 10% negative autotropism implemented, and branching and growth limited to localities where there are less than 8 and 15 neighbouring tips, respectively, in a radius of 20 length units around the growing tip, and branching occurring with a probability of 80% per time unit. Furthermore, growth and branching of tips are each stopped when the tips reach an age of 10 time units. Figure 12) *Spider*: Stage 1: Run for 200 time units at a growth rate of 1 length unit per time unit, with 10% negative autotropism implemented, and the density field hypothesis of branching regulation applied, where the density field threshold for branching is set at 0.1 and branching probability at 80% per time unit. Stage 2: Run for 100 time units at a growth rate of 1 length unit per time unit, with 10% negative autotropism implemented, and branching and growth limited to localities where there are less than 50 and 80 neighbouring tips, respectively, in a radius of 50 length units around the growing tip, and branching occurring with a probability of 80% per time unit. Furthermore, growth and branching of tips are each stopped when the tips reach an age of 20 time units. Figure 13) *Parent and daughter mycelia*: Stage 1: Run for 200 time units at a growth rate of 1 length unit per time unit, with 10% negative autotropism implemented, and the density field hypothesis of branching regulation applied, where the density field threshold for branching is set at 0.06 and branching probability at 40% per time unit (*Tricholomas* parameter set). Stage 2: Run for 100 time units at a growth rate of 1 length unit per time unit, with 10% negative autotropism implemented, and growth limited to localities where there are less than 135 neighbouring tips in a radius of 100 length units around the growing tip, and branching occurring with a probability of 0.1% per time unit. Stage 3: Run for 100 time units at a growth rate of 0.5 length unit per time unit, with 10% negative autotropism implemented, and branching and growth limited to localities where there are less than 100 and 150 neighbouring tips, respectively, in a radius of 100 length units around the growing tip, and branching occurring with a probability of 80% per time unit. Figure 14) *Doughnut*: Stage 1: Run for 90 time units at a growth rate of

Figure legend continued on next page

Figures 10-15. Legend continued.
1 length unit per time unit, with no negative autotropism implemented, and the density field hypothesis of branching regulation applied, where the density field threshold for branching is set at 0.1 and branching probability at 80% per time unit. Stage 2: Run for 110 time units at a growth rate of 1 length unit per time unit, with no negative autotropism implemented, and the density field hypothesis of branching regulation applied, where the density field threshold for branching is set at 0.005 and branching probability at 20% per time unit. Furthermore, branching is stopped when the tips reach an age of 50 time units. Stage 3: Run for 30 time units at a growth rate of 1 length unit per time unit, with no negative autotropism implemented, and the density field hypothesis of branching regulation applied, where the density field threshold for branching is set at 0.5 and branching probability at 80% per time unit. Furthermore, growth is stopped when the tips reach an age of 25 time units. Figure 15) *Rod*: Run for 1000 time units at a growth rate of 1 length unit per time unit, with no negative autotropism implemented, and the density field hypothesis of branching regulation applied, where the density field threshold for branching is set at 0.005 and branching probability at 80% per time unit.

more star-like than spherical. We wish to emphasise that this remarkable differentiation of hyphae emerges in the visualisation even though the program does not include routines implementing differences in hyphal behaviour. In the mathematical model all virtual hyphae are driven by the same algorithm. By altering the persistence factor, it is possible to generate the whole range of intermediate forms between *Boletus* and *Amanita* types.

Finally, when both autotropic reaction and branching are regulated by the hyphal density field, a spherical, uniformly dense colony is also formed. However, the structure is different again, such a colony being similar to the *Tricholoma* type illustrated by Fries[43](Figs. 6 & 9). This type has the appearance of a dichotomous branching pattern, but it is not a true dichotomy. Rather the new branch, being very close, generates a strong density field that turns the older tip. In the previous model a tip nearby has no stronger effect than a more distant tip as long as they are both closer than R.

Hence the *Amanita rubescens* and *Tricholoma* branching strategies may be based on a negative autotropic reaction of the growing hyphae while the *Boletus* strategy may be based on the absence of such a reaction, relying only on density-dependent branching. Differences between *Amanita* and *Tricholoma* in the way that the growing tip senses its neighbours may be obscured in life. In *Amanita* and *Boletus* types, the tip may sense the number of other tips in its immediate surroundings. In the *Tricholoma* type, the tip may sense all other parts of the mycelium, but the local segments have the greatest impact.

Our models show that the broadly different types of branching observed in the fungal mycelium are likely to be based on differential expression of relatively simple control mechanisms. We presume that the "rules" governing branch patterning (that is, the mechanisms causing the patterning) are likely to change in the life of a mycelium, as both intracellular and extracellular conditions alter. We have imitated some of these changes by making alterations to particular model parameters during the course of a simulation. Some of the results are illustrated in Figures 10-15, and they show that the Neighbour-Sensing model is capable of generating a range of morphologies in its virtual mycelia which are reminiscent of fungal tissues. These experiments make it evident that it is not necessary to impose complex spatial controls over development of the mycelium to achieve particular geometrical forms. Rather, geometrical form of the mycelium emerges as a consequence of the operation of specific locally-effective hyphal tip interactions. We hope that further experimentation with the model will enable us to predict how tissue branching patterns are established in real life.

Acknowledgement

LJMcN thanks the British Mycological Society for the award of a Bursary that enabled his contribution to this chapter.

References

1. Adams HL, Thomas CR. The use of image analysis for morphological measurements on filamentous organisms. Biotechnol Bioeng 1988; 32:707-712.
2. Money NP. The pulse of the machine - reevaluating tip-growth methodology. New Phytologist 2001; 151:553-555.
3. Jackson SL. Do hyphae pulse as they grow? New Phytologist 2001; 151:556-560.
4. Hammad F, Watling R, Moore D. Artifacts in video measurements cause growth curves to advance in steps. J Microbiol Meth 1993; 18:113-117.
5. Acuña G, Giral R, Agosin E et al. A neural network estimator for total biomass of filamentous fungi growing on two dimensional solid substrate. Biotech Tech 1998; 17(7):515-519.
6. Desgranges C, Vergoignan C, Georges M et al. Biomass estimation in solid state fermentation. I. Manual biochemical methods. Appl Microbiol Biotechnol 1991; 35(2):200-205.
7. Desgranges C, Vergoignan C, Georges M et al. Biomass estimation in solid state fermentation. II. On-line measurements. Appl Microbiol Biotechnol 1991; 35(2):206-209.
8. Katz D, Goldstein D, Rosenberger RF. Model for branch initiation in Aspergillus nidulans based on measurement of growth parameters. J Bacteriology 1972; 109:1097-1100.
9. Trinci APJ. A study of the kinetics of hyphal extension and branch initiation of fungal mycelia. J Gen Microbiol 1974; 81:225-236.
10. Steele GC, Trinci APJ. The extension zone of mycelial hyphae. New Phytologist 1975; 75:583-587.
11. Pirt SJ. A kinetic study of the mode of growth surface colonies of bacteria and fungi. J Gen Microbiol 1967; 47:181-197.
12. Trinci APJ. Influence of the peripheral growth zone on the radial growth rate of fungal colonies. J Gen Microbiol 1971; 67:325-344.
13. Prosser JI, Trinci APJ. A model for hyphal growth and branching. J Gen Microbiol 1979; 111:153-164.
14. Bartnicki-Garcia S. Fundamental aspects of hyphal morphogenesis. Symposia of the Society of General Microbiology 1973; 23:245-267.
15. Trinci APJ. The duplication cycle and branching in fungi. In: Burnett JH, Trinci APJ, eds. Fungal Walls and Hyphal Growth. Cambridge, UK: Cambridge University Press; 1979:319-358.
16. Yang H, King R, Reichl U et al. Mathematical model for apical growth, septation, and branching of mycelial microorganisms. Biotechnol Bioeng 1992;39:49-58.
17. Leopold LB. Trees and streams: The efficiency of branching patterns. J Theor Biol 1971; 31:339-354.
18. Horton RE. Erosional development of streams and their drainage basins: Hydrophysical approach to quantitative morphometry. Bull Geographical Soc Amer 1945; 56:275-370.
19. Gull K. Mycelium branch patterns of Thamnidium elegans. Transactions of the British Mycological Society 1975; 64:321-324.
20. Obert M, Pfeifer P, Sernetz M. Microbial growth patterns described by fractal geometry. J Bacteriol 1990; 172:1180-1185.
21. Ritz K, Crawford J. Quantification of the fractal nature of colonies of Trichoderma viride. Mycol Res 1990; 94:1138-1152.
22. Jones CL, Lonergan GT, Mainwaring DE. A rapid method for the fractal analysis of fungal colony growth using image processing. Binary 1993; 5:171-180.
23. Matsuura S, Miyazima S. Colony of the fungus Aspergillus oryzae and self-affine fractal geometry of growth fronts. Fractals 1993; 1:11-19.
24. Cohen D. Computer simulation of biological pattern generation processes. Nature 1967; 216:246-248.
25. Hutchinson SA, Sharma P, Clarke KR et al. Control of hyphal orientation in colonies of Mucor hiemalis. Transactions of the British Mycological Society 1980; 75:177-191.
26. Robinson PM. Chemotropism in fungi. Transactions of the British Mycological Society 1973; 61:303-313.
27. Robinson PM. Autotropism in fungal spores and hyphae. Botanical Rev 1973; 39:367-384.
28. Trinci APJ, Saunders PT, Gosrani R et al. Spiral growth of mycelial and reproductive hyphae. Transactions of the British Mycological Society 1979; 73:283-292.
29. Indermitte C, Liebling TM, Clémençon H. Culture analysis and external interaction models of mycelial growth. Bull Mathematical Biol 1994; 56(4):633-664.
30. Edelstein L. The propagation of fungal colonies: A model for tissue growth. J Theor Biol 1982; 98:679-701.
31. Ferret E, Siméon JH, Molin P et al. Macroscopic growth of filamentous fungi on solid substrate explained by a microscopic approach. Biotechnol Bioeng 1999;65(5):512-522.
32. Koch KL. The kinetics of mycelial growth. J General Microbiol 1975; 89:209-216.

33. Monod J. The growth of bacterial cultures. Ann Rev Microbiol 1949; 3:371-394.
34. Edelstein L, Segel LA. Growth and metabolism in mycelial fungi. J Theor Biol 1982; 104:187-210.
35. Mitchell DA, Do DD, Greenfield PF. A semimechanistic mathematical model for growth of Rhizopus oligosporus in a model solid-state fermentation system. Biotechnol Bioeng 1991; 38(4):353-362.
36. Bartnicki-Garcia S, Hergert F, Gierz G. Computer simulation of fungal morphogenesis and the mathematical basis of hyphal (tip) growth. Protoplasma 1989; 153:46-57.
37. Gierz G, Bartnicki-Garcia S. A three-dimensional model of fungal morphogenesis based on the vesicle supply center concept. J Theor Biol 2001; 208(2):151-164.
38. Trinci APJ. Regulation of hyphal branching and hyphal orientation. In: Jennings DH, Rayner ADM, eds. Ecology and Physiology of the Fungal Mycelium. Cambridge, UK: Cambridge University Press; 1984:23-52.
39. Trinci APJ, Wiebe MG, Robson GD. The mycelium as an integrated entity. In: Wessels JGH, Meinhardt F, eds. Growth, Differentiation and Sexuality. (The Mycota, vol. 1). Berlin, Heidelberg: Springer-Verlag; 1994:175-193.
40. Moore D. Tissue Formation. In: Gow NAR, Gadd GM, eds. The Growing Fungus. London: Chapman & Hall; 1994:423-465.
41. Chiu SW, Moore D. Patterns in Fungal Development. Cambridge, U.K.: Cambridge University Press; 1996.
42. Moore D. Fungal Morphogenesis. New York: Cambridge University Press; 1998.
43. Fries N. Untersuchungen über Sporenkeimung und Mycelentwicklung bodenbewohneneder Hymenomyceten. Symbolae Botanicae Upsaliensis 1943; 6(4):633-664.
44. Kotov V, Reshetnikov SV. A stochastic model for early mycelial growth. Mycol Res 1990; 94:577-586.
45. Hogeweg P, Hesper B. A model study on biomorphological description. Pattern Recognition 1974; 6:165-179.
46. Witten IH, Frank E. Data Mining: Practical Machine Learning Tools and Techniques with Java Implementations. San Francisco: Morgan Kaufmann Publishers; 1999.